

## SCALING RELATIONSHIPS OF SOURCE PARAMETERS OF INLAND CRUSTAL EARTHQUAKES IN TECTONICALLY ACTIVE REGIONS

K. MIYAKOSHI<sup>1</sup>, K. SOMEI<sup>1</sup>, K. IRIKURA<sup>2</sup>, K. KAMAE<sup>3</sup>

<sup>1</sup>Geo-Research Institute (GRI), Osaka, Japan

<sup>2</sup>Aichi Institute of Technology (AIT), Toyota, Japan

<sup>3</sup>Kyoto University Research Reactor Institute (KURRI), Kumatori, Japan

*E-mail contact of main author: ken@geor.or.jp*

**Abstract.** A three-stage scaling relationship between source rupture area and seismic moment of the inland earthquakes proposed by Irikura and Miyake (2011) and revised by Murotani *et al.* (2015), based on waveform inversion results using strong motion data and teleseismic data of inland crustal earthquakes occurring mostly in California, USA. In this study, we recognized that the scaling relationship of rupture area versus seismic moment coincides with the three-stage source scaling relationship using source parameters extracted from waveform inversions of 25 recent inland crustal earthquakes in Japan ( $M_w$ 5.4-7.1). The scaling relationship between rupture area and seismic moment has been proposed by a substantial number of studies. The rupture areas have been highly accurately estimated by waveform inversion analyses rather than aftershock distribution or surface rupture surveys after earthquakes. However, the different approaches of the waveform inversion analysis possibly result in variability of rupture area. Therefore, it is necessary to use consistent criteria to evaluate rupture area based on heterogeneous slip distributions. In this study we compiled rupture areas trimmed by the criterion of Somerville *et al.* (1999). We compared the rupture area trimmed by another criterion of Thingbaijam and Mai (2016) with the common 24 slip models (Thingbaijam *et al.*, 2017). Consequently, both trimmed rupture areas agree well each other. Scaling relationships of source parameters are found to depend on the seismotectonic regime and faulting style. Therefore, we categorize rupture models according to the same seismotectonic setting in active regions such as Japan or Southern California, USA. Japanese archipelago is classified into the crustal intraplate regions close to active plate margin, where seismicity is very high. Depend on the thickness of seismogenic zone, the fault width saturate at about 16-18km for inland crustal earthquakes. We recognized that fault widths also saturate larger than  $M_w$ 6.5 for crustal interplate earthquakes for strike-slip in active seismic regions such as west USA compiled from the SRCMOD database.

**Key Words:** Three-stage scaling relationship, earthquake category, waveform inversion, trimming method.

### 1. INTRODUCTION

After the 1995 Hyogo-ken Nanbu earthquake ( $M_w$ 6.9) in Japan, dense strong ground motion networks (K-NET, KiK-net) were installed at about 20 km intervals by NIED (National Research Institute for Earth Science and Disaster Resilience). Using strong ground motions near the source region, many heterogeneous slip models could be estimated by waveform inversion analysis with high accuracy velocity structure models. Source parameters (rupture area, average slip, and asperity area etc.) are extracted from heterogeneous slip models using certain criteria, and empirical scaling relationships between source parameters and seismic moment are evaluated by regression analysis. A three-stage source scaling relationship between source rupture area and seismic moment of inland crustal earthquakes has been

initially proposed by Irikura and Miyake (2011)<sup>[1]</sup> and revised by Murotani *et al.* (2015)<sup>[2]</sup>. Fig.1 shows the schematic source model for each stage. For the first stage,  $S$  is proportional to  $Mo^{2/3}$  (self-similar scaling) for earthquakes smaller than around  $M_w 6.5$  (Somerville *et al.*, 1999<sup>[3]</sup>). For the second stage,  $S$  is proportional to  $Mo^{1/2}$  (the saturation of width for the limited thickness of seismogenic zone) for earthquakes between around  $M_w 6.5$  and 7.4 (Irikura and Miyake, 2011<sup>[1]</sup>). For the third stage,  $S$  is proportional to  $Mo$  (the saturation of the slip) for earthquakes larger than around  $M_w 7.4$  (Tajima *et al.*, 2013<sup>[4]</sup>; Murotani *et al.*, 2015<sup>[5]</sup>). The Headquarters for Earthquake Research Promotion (HERP, 2017<sup>[6]</sup>) in Japan adopts such three-stage source scaling relationship for predicting of strong ground motions for identified earthquake scenarios. However, some researchers (e.g., Wells and Coppersmith, 1994<sup>[7]</sup>; Leonard, 2010<sup>[8]</sup>) proposed the self-similar scaling relationship ( $S$  is proportional to  $Mo^{2/3}$ ) and Hanks and Bakun (2002)<sup>[9]</sup> proposed a two-stage scaling relationship ( $S$  is proportional to  $Mo^{2/3}$  and  $Mo^{1/2}$ ) for the limited thickness of seismogenic zone.

There are suggestions that source scaling is affected by the tectonic regionality and focal mechanism. Stirling *et al.* (2013)<sup>[10]</sup> proposed different source scaling relationship according to tectonic regime (e.g., plate boundary crustal, stable continental, subduction, and volcanic). Wells and Coppersmith (1994)<sup>[7]</sup> indicate that surface rupture length observed from geological survey and subsurface rupture length estimated from the best-defined aftershock zone are not necessarily consistent with each other. So, it is possible that dataset reliability of source parameters estimated from different measurements affects the source scaling relationship. To discuss the source scaling relationship accurately, we need to use source parameters of earthquakes estimated using the same measurement technique in the same tectonic regionality. In this study we consider fault rupture models estimated from waveform inversion analysis because we believe that they contribute the most accurate estimates of “true” fault dimensions by the trimming method (e.g., Somerville *et al.*, 1999<sup>[3]</sup>; Thingbaijam and Mai, 2016<sup>[11]</sup>). We have recognized that inland crustal earthquakes in and around Japan are categories in the same tectonic regionality as Southern California, USA, because of the saturation of rupture width (e.g., Irikura and Miyake, 2011<sup>[1]</sup>; Leonard, 2010<sup>[8]</sup>). So we investigate source scaling relationships of inland crustal earthquakes in tectonically active regions using source parameters obtained from rupture models by waveform inversion analysis.

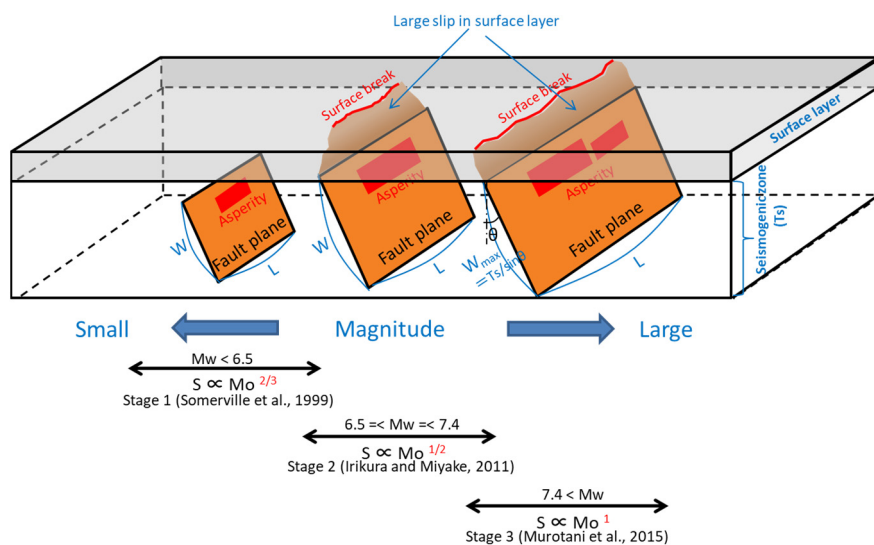


FIG. 1. Schematic source model for each scaling stage

## 2. EARTHQUAKE CATEGORIZATION

Earthquakes occur in different seismotectonic settings and involve various types of source mechanism. First of all, the seismotectonic setting needs to be identified for discussion of source scaling relationships. The new regulatory guides of NRA (Nuclear Regulation Authority in Japan) categorize earthquakes into three types (inland crustal earthquakes, interplate earthquakes and oceanic intraplate earthquakes). Our main targets are the inland crustal earthquakes in tectonically active regions in Japan and Southern California, USA, so we categorized the inland crustal earthquakes compiled by Somerville *et al.* (1999)<sup>[3]</sup> and Miyakoshi *et al.* (2015)<sup>[12]</sup> referring to the seismotectonic regime of IAEA (2016)<sup>[13]</sup>. We propose earthquake categorization for the inland crustal earthquakes in tectonically active regions as shown in Fig.2. Firstly, we divide the earthquakes into two categories, subduction and non-subduction earthquakes, according to the plate tectonic setting. Subduction earthquakes occur along the subduction interface, in-slab, and outer-rise. Secondly, we divide the non-subduction earthquakes category into oceanic and continental earthquakes. We do this because thickness is expected to differ between ocean and continental crusts owing to isostasy. Thirdly, the continental earthquakes category is divided between stable region and active region earthquakes in Japan and Southern California, USA. The stable region is as same as the SCR (Stable Continental Region; Wells and Coppersmith, 1994<sup>[7]</sup>). Active region earthquakes include intraplate (inland crustal; e.g., 2016 Kumamoto, Japan, earthquake), transform interplate (e.g., 1989 Loma Prieta, California, earthquake), and thrust interplate earthquakes with low dipping angle (e.g., 2015 Gorkha, Nepal, earthquake) as shown in Fig.2. Our target earthquake category for the source scaling relationship is the inland crustal earthquake, which includes intraplate and transform interplate earthquakes except for thrust interplate earthquakes.

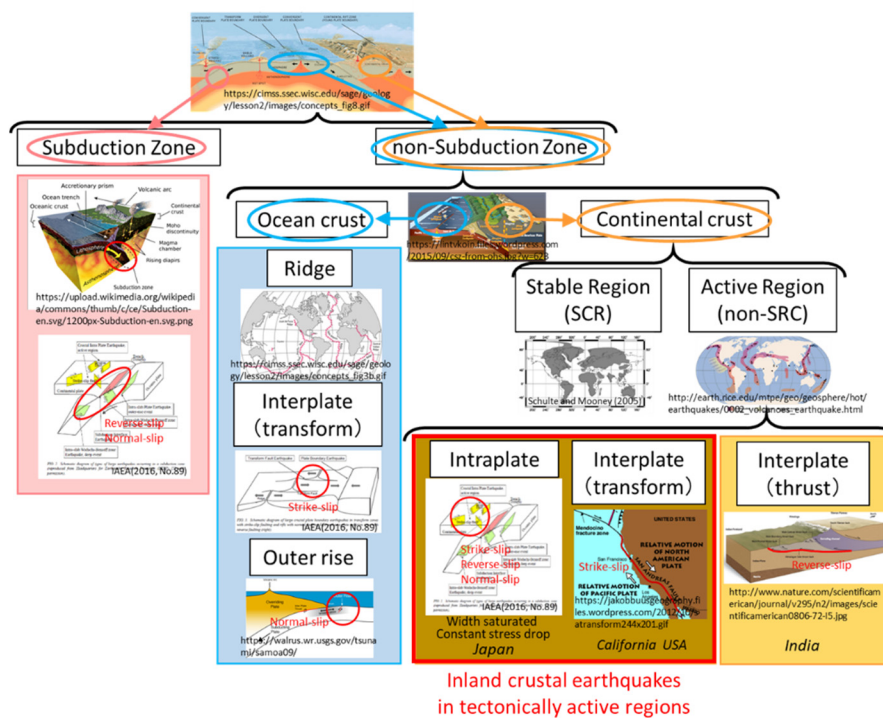


FIG. 2. Earthquake category for inland crustal earthquakes in tectonically active regions (red rectangle)

### 3. WAVEFORM INVERSION RESULTS

Using the waveform inversion results of 25 recent inland crustal earthquakes ( $M_w 5.4 - 7.1$ ) (see Fig.3), which occurred in Japan after the 1995 Hyogo-ken Nanbu earthquake ( $M_w 6.9$ ), we extracted the source parameters from the inversion results using the same criterion by Somerville *et al.* (1999)<sup>[3]</sup>. These seismic magnitude ranges ( $M_w 5.4 - 7.1$ ) correspond to the first or second stage for the three-stage source scaling relationship. Fig.4 shows an example of the waveform inversion result of the 2016 Ibaraki-ken Hokubu, Japan, earthquake ( $M_w 5.9$ ). The black rectangle and red rectangle in Fig.4 show rupture area and asperity area extracted from the final slip distribution using the same criterion by Somerville *et al.* (1999)<sup>[3]</sup>. In most waveform inversion analysis, the rectangular dimensions of the fault are chosen to be at least large enough to accommodate the entire fault rupture estimated from the best-defined aftershock zone and so they sometimes overestimate the actual dimensions of the rupture area. To estimate “true” fault dimension accurately, Somerville *et al.* (1999)<sup>[3]</sup> trimmed slip models by removing rows/columns if their average slip is less than 0.3 times average slip in rupture area. Mai and Beroza (2000)<sup>[14]</sup> introduced the concept of effective source dimensions, based on the autocorrelation width of the spatially variable slip. Thingbaijam *et al.* (2017)<sup>[15]</sup> also trimmed slip models by using a new concept of effective source dimensions (Thingbaijam and Mai, 2016<sup>[11]</sup>) extended from Mai and Beroza (2000)<sup>[14]</sup>. Because both trimming methods have the common purpose of estimating “true” fault dimension accurately, we need to evaluate whether the same source parameters are extracted. Next, we compare the trimming method between Somerville *et al.* (1999)<sup>[3]</sup> and Thingbaijam and Mai (2016)<sup>[11]</sup>.

We selected the common 11 slip models of inland crustal earthquakes that occurred in Japan which are compiled by Miyakoshi *et al.* (2015)<sup>[12]</sup> and Thingbaijam *et al.* (2017)<sup>[15]</sup>. The former used the Somerville *et al.* (1999)<sup>[3]</sup>'s trimming method and the latter used Thingbaijam and Mai (2016)<sup>[11]</sup>'s method. Fig.5 shows the comparison of source parameters extracted from slip models by the different trimming methods. The common 13 slip models of inland crustal earthquakes that mainly occurred in Southern California, USA, compiled by Somerville *et al.* (1999)<sup>[3]</sup> and Thingbaijam *et al.* (2017)<sup>[15]</sup> are also plotted in Fig.5. We recognized that source parameters extracted from slip models by the different trimming methods consistent each other except for some earthquakes. Although rupture areas trimmed by Somerville *et al.* (1999)<sup>[3]</sup> are smaller than those by Thingbaijam and Mai (2016)<sup>[11]</sup>, discrepancy is small, attaining about 0.2 (log-scale) at the maximum. It is important to note that the different trimming methods of Somerville *et al.* (1999)<sup>[3]</sup> and Thingbaijam and Mai (2016)<sup>[11]</sup> give almost the same source parameters. Thus, trimmed slip models of Somerville *et al.* (1999)<sup>[3]</sup>, Miyakoshi *et al.* (2015)<sup>[12]</sup>, and Thingbaijam *et al.* (2017)<sup>[15]</sup> represent the best-resolved attribute source properties and have been used to investigate accurately the source rupture scaling.

Fig.6(a), (b) show the relationships between rupture area ( $A$ ) and seismic moment ( $M_o$ ) and between rupture length ( $L$ ) and seismic moment ( $M_o$ ), respectively. We recognized that these source parameters versus seismic moment ( $A-M_o$  or  $L-M_o$ ) in this study are in good agreement with the three-stage source scaling relationship (HERP, 2017)<sup>[6]</sup>. The other empirical scaling relationships (Hanks and Bakun, 2002<sup>[9]</sup>; Leonard, 2010<sup>[8]</sup>; Thingbaijam *et al.*, 2017<sup>[15]</sup>) also consist with the estimated source parameters. We conclude that a clear dependence of the source mechanism type on source parameters cannot be seen in these figures. Fig.6(c) shows the relationship between rupture width ( $W$ ) and seismic moment ( $M_o$ ).

Rupture widths estimated from inversion results are in good agreement with the bilinear source scaling relationship ( $W$ - $M_o$ ) by Leonard (2010)<sup>[8]</sup> or Irikura and Miyake (2011)<sup>[11]</sup>. It is obvious that rupture widths are saturated at 16-18km ( $M_w \geq 6.5 - 7$ ) for the thickness of the seismogenic zone in Fig.6(c). However, Thingbaijam *et al.* (2017)<sup>[15]</sup> propose that rupture width becomes longer with increasing seismic moment and does not saturate in case of the inland crustal earthquakes with strike-slip. Later, we will discuss whether rupture width saturates for the inland crustal earthquakes. Fig. 6(d) shows the relationship between the combined areas of asperities ( $A_{asp}$ ) and seismic moment ( $M_o$ ). The combined areas of asperities are an important source parameter corresponding to the effective stress drop for the prediction of strong ground motions (HERP, 2017)<sup>[6]</sup>. We recognized that the slope for the scaling relationship between the combined areas of asperities and seismic moment in this study coincides with that of Somerville *et al.* (1999)<sup>[3]</sup>.

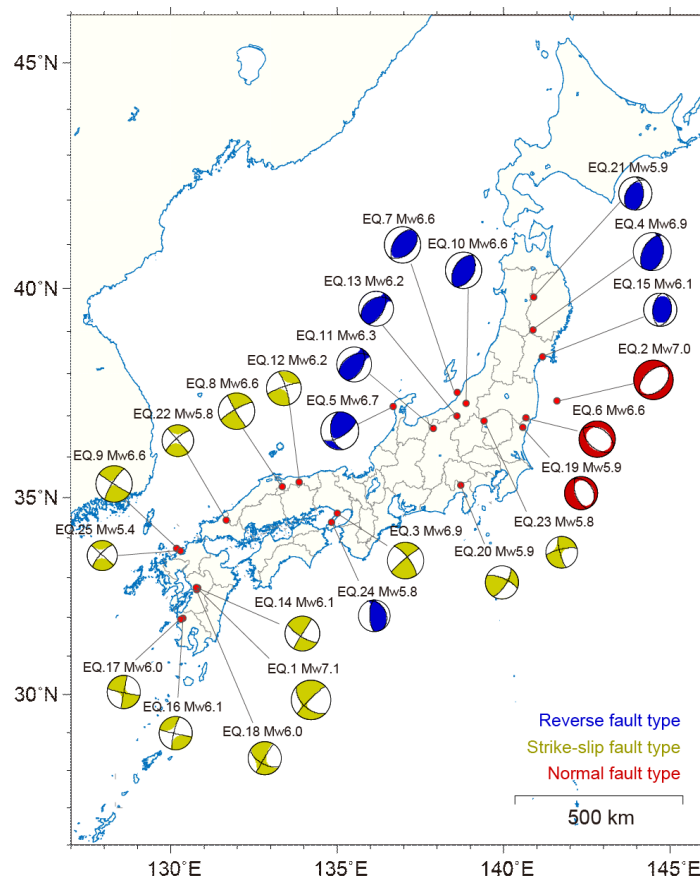


FIG. 3. Distribution of 25 events included in this study and their focal mechanisms (F-net)

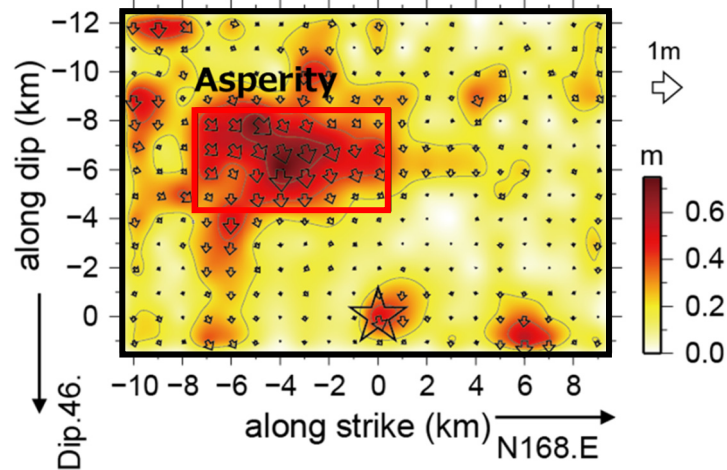


FIG. 4. Slip distribution on fault plane of the 2016 Ibaraki-ken Hokubu, Japan, earthquake ( $M_w$ 5.9). Star indicates the hypocenter. Red rectangle is the asperity area extracted from the final slip distribution using the same criterion by Somerville et al. (1999).

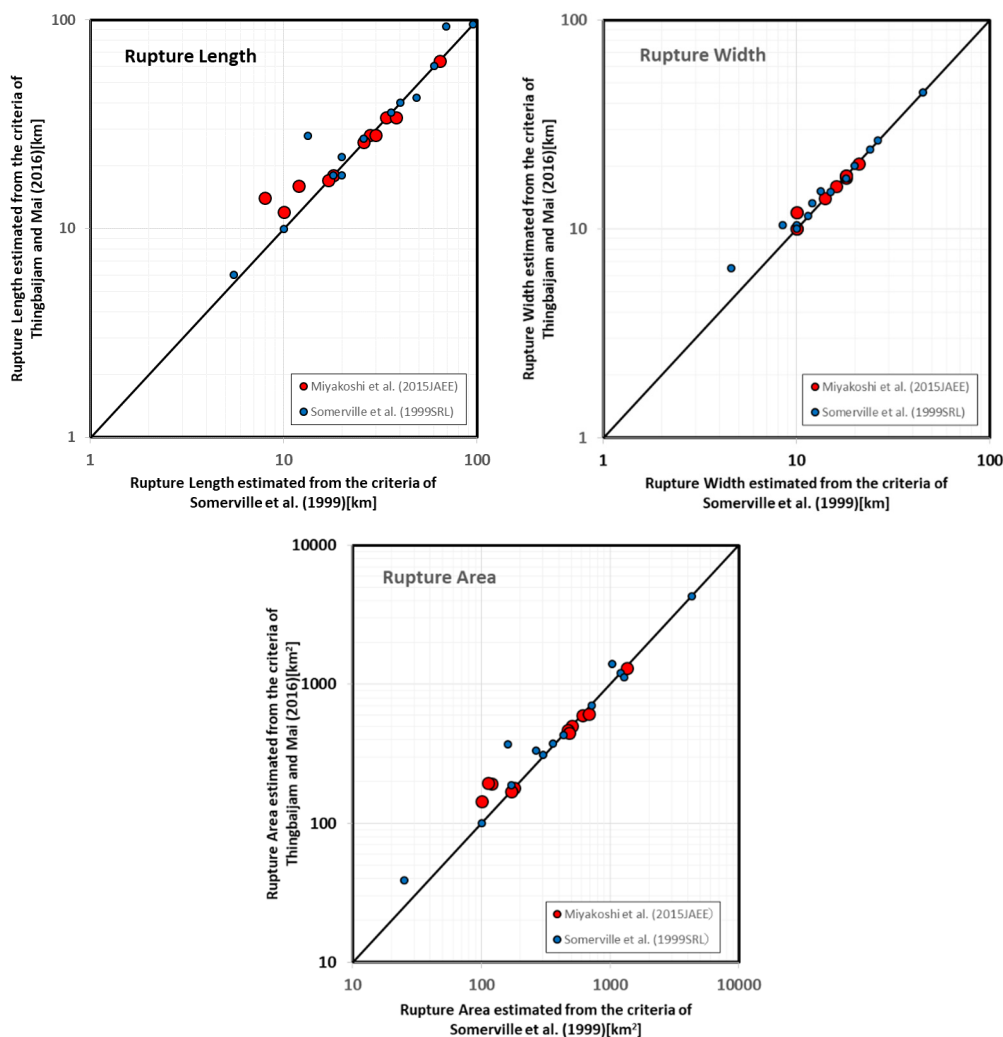


FIG. 5. Comparison between source parameters of slip model trimmed by the criteria of Somerville et al. (1999) and Thingbaijam & Mai (2016). Red and blue circles are source parameters compiled by Miyakoshi et al. (2015) and Somerville et al. (1999), respectively.

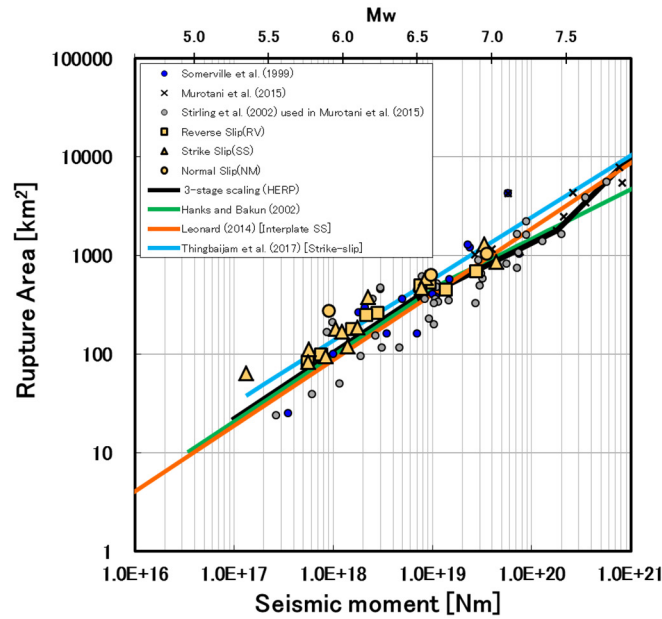


FIG. 6(a). Relationship between rupture area and seismic moment. Yellow symbols denote earthquakes included in this study. (Square: reverse-slip, Triangle: strike-slip, Circle: normal-slip)

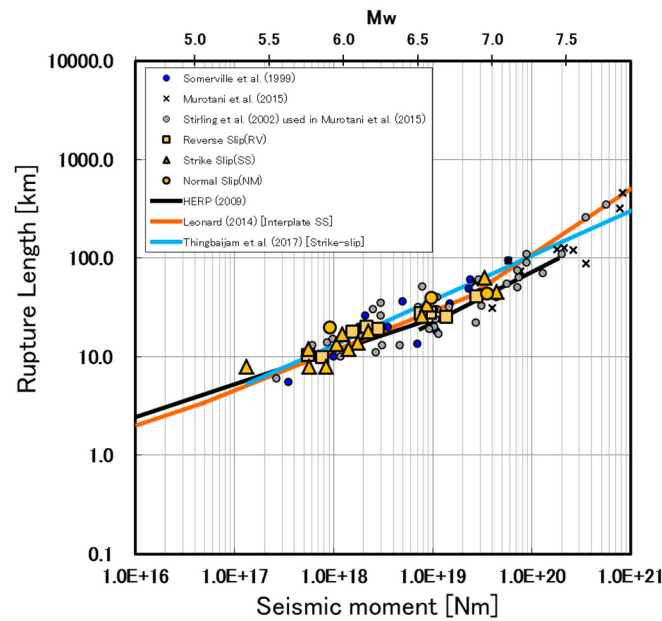


FIG. 6(b). Relationship between rupture length and seismic moment. Yellow symbols denote earthquakes included in this study. (Square: reverse-slip, Triangle: strike-slip, Circle: normal-slip)

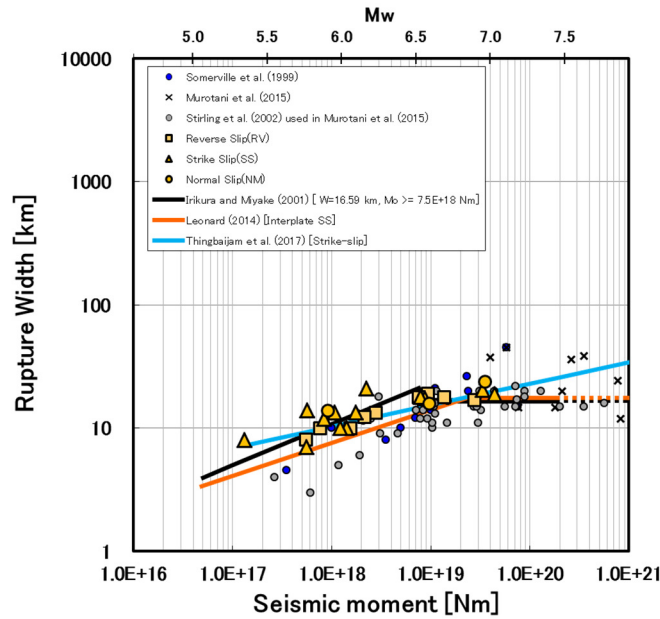


FIG. 6(c). Relationship between rupture width and seismic moment. Yellow symbols denote earthquakes included in this study. (Square: reverse-slip, Triangle: strike-slip, Circle: normal-slip)

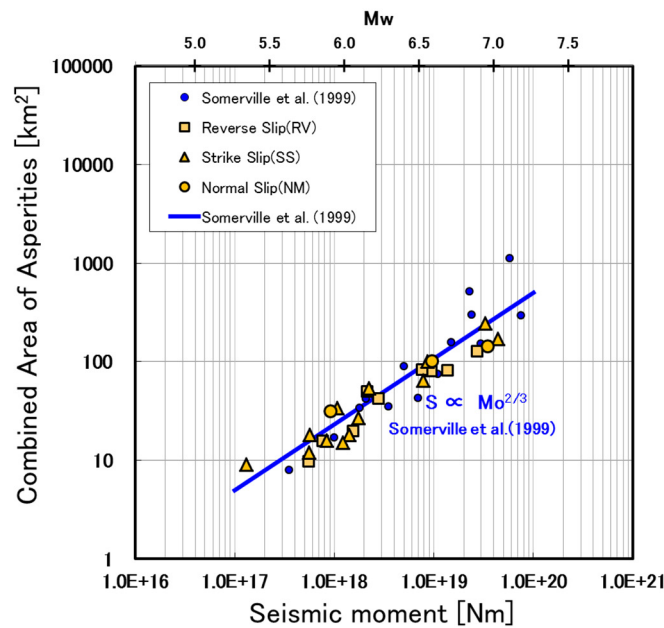


FIG. 6(d). Relationship between combined area of asperities and seismic moment. Yellow symbols denote earthquakes included in this study. (Square: reverse-slip, Triangle: strike-slip, Circle: normal-slip)



Fig.7 shows the distributions of residuals between the estimated rupture areas of 25 inland crustal earthquakes and predicted ones with respect to seismic moment (or  $M_w$ ). Panels (a) in Fig. 7 denote the self-similar scaling relationships and (b) denote the bended (two- or three-stage) ones (see Fig.6(a)). Red solid line shows the mean residual and brown dash line shows its standard deviation. Vertical thick grey line in (b) denotes the transition moment magnitude ( $M_w$ ) from the first to second stage scaling. The scaling relationship of Thingbaijam *et al.* (2017)<sup>[15]</sup> agrees reasonably well with the estimated rupture areas. However, in the moment magnitude range larger than  $M_w$ 6.5, we also recognized mostly negative residuals for this scaling relationship. Fig.8 shows that the mean residuals ( $M_w \geq 6.5$ ) become larger than those ( $M_w < 6.5$ ). As we recognized mostly smaller distributions of residuals for the bended scaling relationships ( $M_w \geq 6.5$ ) in Fig.7(b) (e.g., Hanks and Bakun, 2002<sup>[9]</sup>), it is suggested that two- or three-stage scaling relationships are better than the self-similar ones.

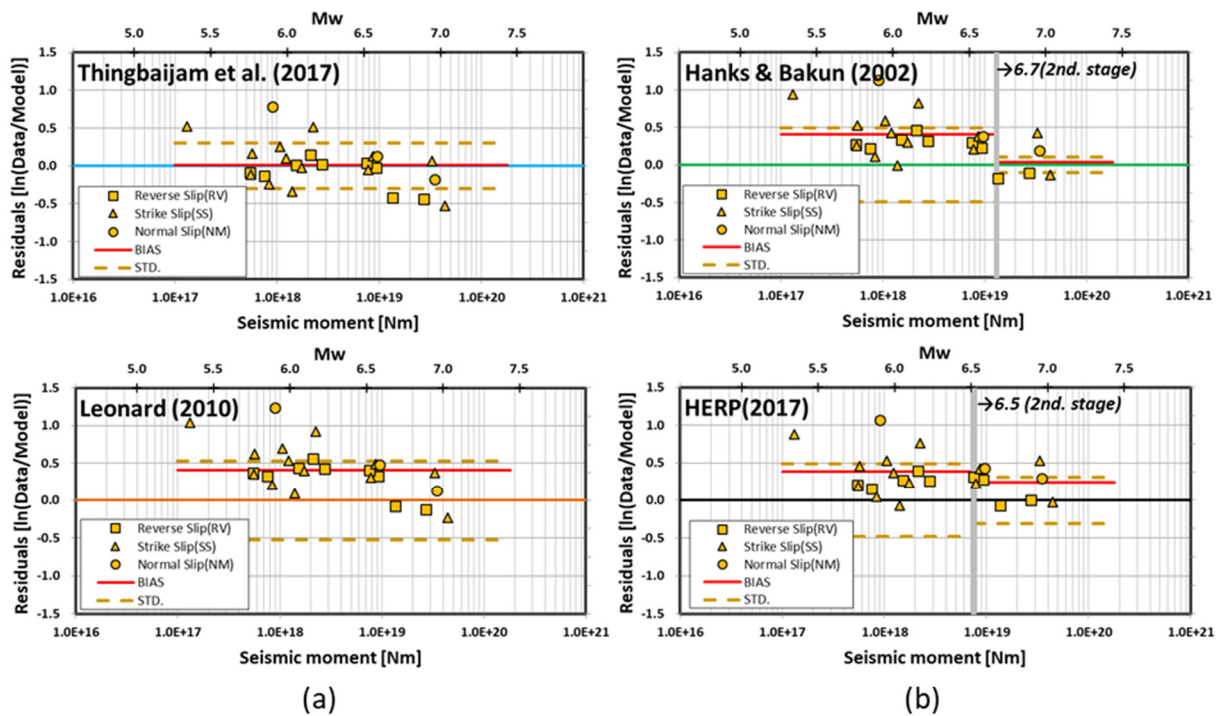


FIG. 7. Distribution of the residuals (difference between estimated rupture areas and predicted ones on natural log scale) with respect to seismic moment (or  $M_w$ ): (a) for self-similar scaling relationship (Thingbaijam *et al.*, 2017; Leonard, 2010) and (b) for second or third-stage scaling relationship (Hanks and Bakun, 2002; HERP, 2017). Red solid line shows the mean residual and brown dash line shows its standard deviation. Vertical thick grey line denotes the transition  $M_w$  from the first to second stage scaling.

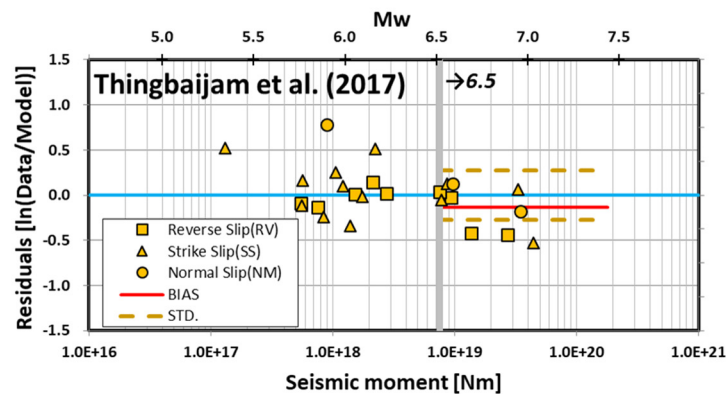


FIG. 8. Distribution of the residuals (difference between estimated rupture areas and predicted ones on natural log scale) with respect to seismic moment (or  $M_w$ ) for the Thingbajam et al. (2017). We assumed transition  $M_w$  6.5 referring to HERP(2017).

## 4. DISCUSSION

### 4.1. AVERAGE STATIC STRESS DROP IN RUPTURE AREA

Source scaling is an important issue for earthquake source physics. Since Aki (1967)<sup>[16]</sup> proposed the seismic scaling law of source spectrum, it has been widely accepted that the stress drop has a constant value independent of seismic moment. Wells and Coppersmith (1994)<sup>[7]</sup> or Leonard (2010)<sup>[8]</sup> proposed the self-similar scaling relationship of constant stress drop ( $S$  is proportional to  $Mo^{2/3}$ ) for a wide seismic moment range. However, HERP (2017)<sup>[6]</sup> adopts the three-stage source scaling relationship with different slope between source rupture area and seismic moment. So, we need to discuss whether stress drop is different for the wide seismic moment range. Using method of Bouchon (1997)<sup>[17]</sup> or Ide and Takeo (1997)<sup>[18]</sup>, we estimated static stress drop in rupture area from heterogeneous slip velocity functions of source inversion results. We also estimated static stress drop in rupture area from heterogeneous final slip of source inversion results by using method of Okada (1992)<sup>[19]</sup>. Fig. 9 shows an example of the static stress drops distribution of the 2016 Ibaraki-ken Hokubu, Japan, earthquake ( $M_w$ 5.9) estimated using the method by Ide and Takeo (1997)<sup>[18]</sup>. Fig. 10 shows the average static stress drop with the seismic moment. Some average static stress drops in the off-asperity area (Iwata *et al.*, 2005<sup>[20]</sup>; Asano and Iwata, 2011<sup>[21]</sup>) are plotted in in Fig.8, these are possibly a little lower than those in the rupture area. So, we need to discuss carefully whether average static stress drops in the rupture area are different. Average static stress drops become higher with increasing seismic moment, but there is not so large difference in range of first and second stage of three-stage source scaling relationship. The average static stress drops (1–4MPa) in this study are almost in agreement with self-similar stress drop (2.3MPa) based on the recipe of HERP (2017)<sup>[6]</sup> ( $M_w < 6.5$ ) and static stress drop (3.1MPa) proposed by Fujii and Matsu'ura (2000)<sup>[22]</sup> for strike-slip type earthquakes ( $M_w \geq$  around 6.5). It is suggested that the average static stress drops vary for a small change of 1 – 4MPa for the three-stage source scaling relationship.

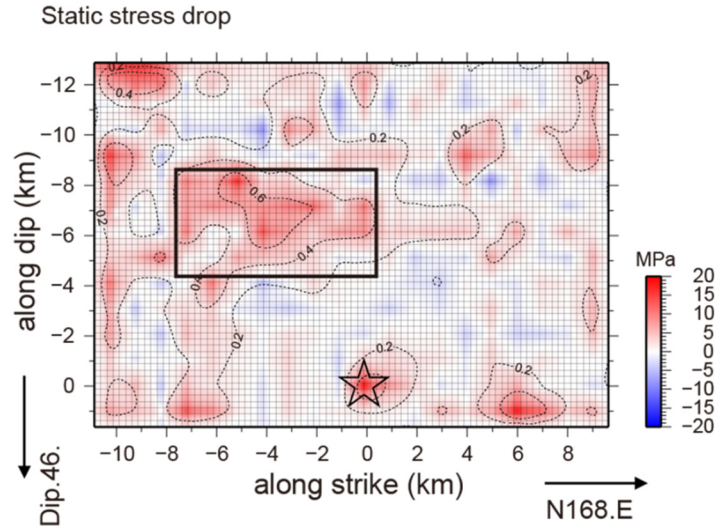


FIG. 9. Static stress drop distribution of the 2016 Ibaraki-ken Hokubu, Japan, earthquake ( $M_w$  5.9) estimated using the method by Ide and Takeo (1997). Star indicates the hypocenter. Black rectangle is asperity area (see FIG. 4).

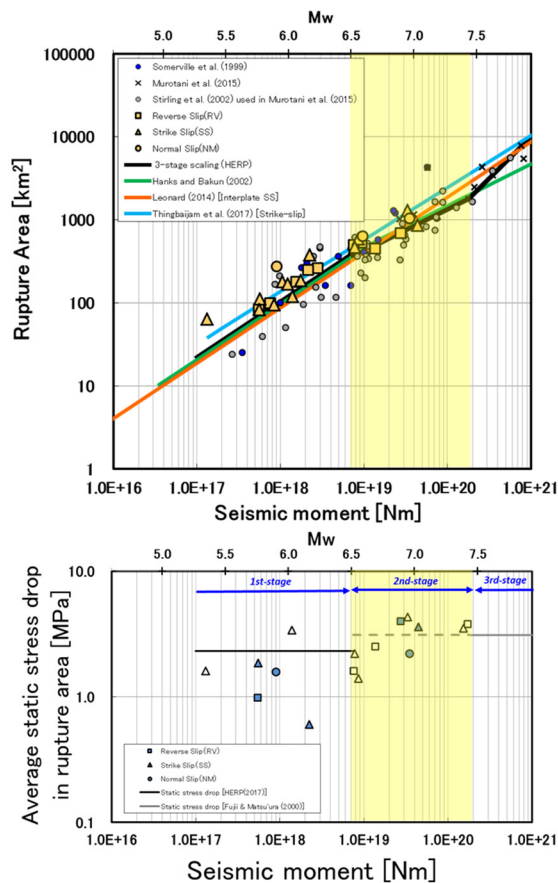


FIG. 10. Relationship between average static stress drop in rupture area and seismic moment. Upper figure shows three-stage source scaling relationship between rupture area and seismic moment. Lower figure shows average static stress drop in rupture area and seismic moment. Open symbols show the average stress drop in the off-asperity area (Iwata et al., 2005; Asano and Iwata, 2011)

## 4.2. SATURATION OF RUPTURE WIDTH

Thingbaijam *et al.* (2017)<sup>[15]</sup> proposed a new scaling relationship for source parameters based on a large SRCMOD database (Mai and Thingbaijam, 2014<sup>[23]</sup>). As mentioned above, they show that rupture width become longer with increasing seismic moment (or  $M_w$ ) and does not saturate for strike-slip type earthquakes (see Fig.6(c)). However, Irikura and Miyake (2011)<sup>[1]</sup> or Leonard (2010)<sup>[8]</sup> proposed that that rupture widths for inland crustal earthquakes (strike-slip, reverse-slip, and normal-slip type) are saturated at about 16-18km for the thickness of the seismogenic zone (see Fig.6(c)). Our compiled inversion results (e.g., Somerville *et al.*, 1999<sup>[3]</sup>; Miyakoshi *et al.*, 2015<sup>[12]</sup>) involve intraplate and transform interplate earthquakes in tectonically active regions mainly in Japan or Southern California, USA (see Fig.2). In contrast, Thingbaijam *et al.* (2017)<sup>[15]</sup> compile strike-slip type earthquakes, which involve oceanic intraplate earthquakes ( $M_w > 7.2$ ) as shown in Fig.11. To discuss the source scaling relationship accurately, it is important to consider earthquakes that occur in the same seismotectonic settings as described above. So, we try to omit the oceanic intraplate earthquakes ( $M_w > 7.2$ ) compiled by Thingbaijam *et al.* (2017)<sup>[15]</sup>. Fig.12 shows the relationship between rupture width ( $W$ ) and seismic moment ( $M_o$ ), which are omitted from the oceanic intraplate earthquakes ( $M_w > 7.2$ ). We recognized that rupture widths are saturated at about 16-18km for inland crustal earthquakes with strike-slip. The database of inland crustal earthquakes from the SRCMOD, except for the oceanic intraplate earthquakes ( $M_w > 7.2$ ), is in good agreement with the empirical scaling relationship of Irikura and Miyake (2011)<sup>[1]</sup> or Leonard (2010)<sup>[8]</sup>.

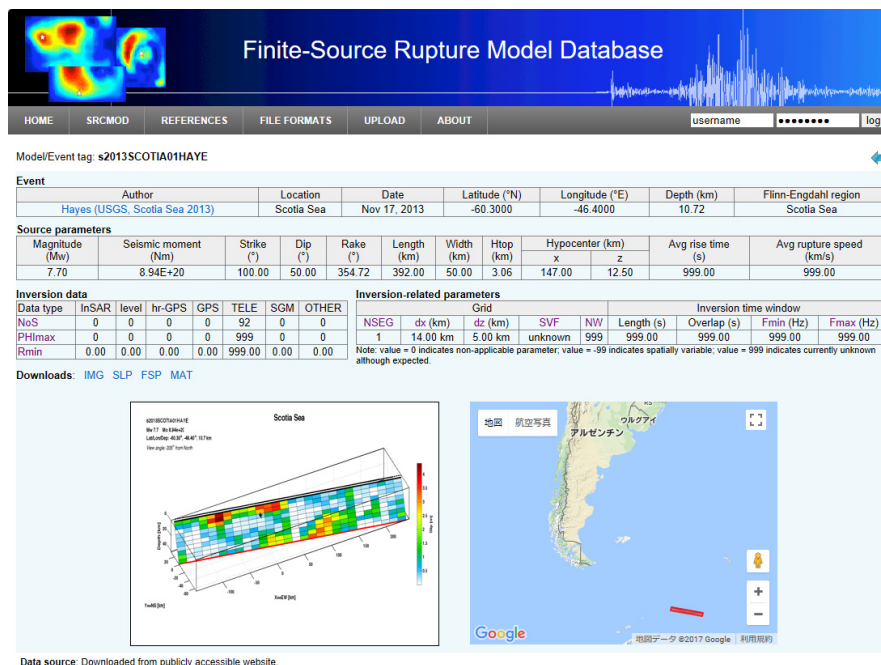


FIG. 11. 2013 Scotia Sea earthquake ( $M_w 7.7$ ) [<http://equake-rce.info/SRCMOD/searchmodels/viewmodel/s2013SCOTIA01HAYE/>]

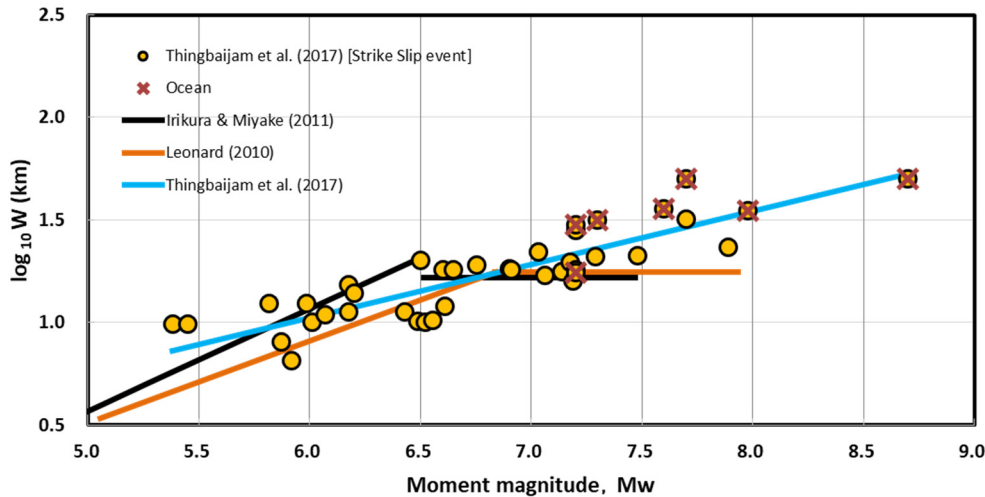


FIG. 12. Relationship between rupture width and moment magnitude for inland crustal earthquakes of strike-slip type. “×” denotes oceanic intraplate earthquakes compiled by Thingbaijam et al. (2017).

## 5. CONCLUSION

Using the waveform inversion results of 25 recent inland crustal earthquakes ( $M_w$  5.4–7.1) in Japan, we extracted the source parameters (rupture area and asperity area etc.) from the inverted heterogeneous slip distributions following the criterion of Somerville *et al.* (1999)<sup>[3]</sup>. We recognized that the scaling relationship of rupture area ( $A$ ) versus seismic moment ( $M_0$ ) obtained in this study coincides with the three-stage source scaling relationship (HERP, 2017)<sup>[6]</sup>. Different trimming methods for the heterogeneous slip model between Somerville *et al.* (1999)<sup>[3]</sup> and Thingbaijam and Mai (2016)<sup>[11]</sup> give almost the same source parameters. It is important to note that the trimmed slip models represent the best-resolved attribute source properties and have been used to accurately investigate the source rupture scaling. We also estimated static stress drop in the rupture area from heterogeneous slip velocity functions or final slip of source inversion results. The average static stress drops (1–4MPa) are almost in agreement with the self-similar stress drops (2.3MPa) based on the recipe of HERP (2017)<sup>[6]</sup> ( $M_w < 6.5$ ) and static stress drop (3.1MPa) proposed by Fujii and Matsu’ura (2000)<sup>[22]</sup> ( $M_w \geq$  around 6.5). Source parameters of rupture width compiled by Thingbaijam *et al.* (2017)<sup>[15]</sup>, except for the oceanic intraplate earthquakes, show saturation at about 16–18km for inland crustal earthquakes with strike-slip. To discuss source scaling relationship, it is important that we use not only the same type of earthquakes but also same the seismotectonic settings.

## 6. ACKNOWLEDGMENTS

We use the hypocentral information catalog of JMA (Japan Meteorological Agency), and the source information from F-net provided by NIED (National Research Institute for Earth Science and Disaster Resilience). We would like to thank Dr. Asano, K. (DPRI), Dr. Sekiguchi, H. (DPRI), Prof. Iwata, T. (DPRI), Dr. Horikawa, H. (AIST), Dr. Kubo, H. (NIED), Dr. Suzuki, W. (NIED), Dr. Aoi, S. (NIED), Dr. Hikima, K. (TEPCO), Dr. Kurahashi, S. (AIT), and Dr. Yoshida, K. (GRI) for provision of waveform inversion results.

This study was based on the 2017 research project ‘Examination for uncertainty of strong ground motion prediction for the inland crustal earthquakes’ by the Nuclear Regulation Authority (NRA), Japan.

## REFERENCES

- [1] IRIKURA, K., and MIYAKE, H., “Recipe for predicting strong ground motion from crustal earthquake scenarios”, *Pure Appl. Geophys.* 168(2011), 85-104.
- [2] MUROTANI, S., et al., “Scaling relation of source parameters of earthquakes on inland crustal mega-fault systems”, *Pure Appl. Geophys.* 172(2015), 1371-1381.
- [3] SOMERVILLE, P., et al., “Characterizing crustal earthquake slip models for the prediction of strong ground motion”, *Seism. Res. Lett.* 70(1999), 59–80.
- [4] TAJIMA, R., et al., “Comparative study on scaling relations of source parameters for great earthquakes in inland crusts and on subducting plate-boundaries”, *ZISIN2 (J. Seismol. Soc. Jpn.)*, 66(2013), 31-45 (in Japanese).
- [5] MUROTANI, S., et al., “Scaling relation of source parameters of earthquakes on inland crustal mega-fault systems”, *Pure Appl. Geophys.*, 172(2015), 1371-1381.
- [6] HEADQUARTERS FOR EARTHQUAKE RESEARCH PROMOTION (HERP), “Predicting strong ground motions for identified earthquake scenarios (RECIPE)”, (2017), (in Japanese). [https://www.jishin.go.jp/main/chousa/17\\_yosokuchizu/recipe.pdf](https://www.jishin.go.jp/main/chousa/17_yosokuchizu/recipe.pdf)
- [7] WELLS, D. L., and COPPERSMITH, K. J., “New empirical relationships among magnitude, rupture length, rupture width, rupture area, and surface displacement”, *Bull. Seismol. Soc. Am.* 84(1994), 974-1002.
- [8] LEONARD, M., “Earthquake fault scaling: Self-consistent relating of rupture length, width, average displacement, and moment release”, *Bull. Seismol. Soc. Am.* 100(2010), 1971-1988.
- [9] HANKS, T. H., and BAKUN, W. H., “A bilinear source-scaling model for M-logA observation of continental earthquakes”, *Bull. Seismol. Soc. Am.* 92(2002), 1841-1846.
- [10] STIRLING, M. T., et al., “Selection of earthquake scaling relationships for seismic-hazard analysis”, *Bull. Seismol. Soc. Am.* 103(2013), 1-19.
- [11] THINGBAIJAM, K. K. S., and MAI, P. M., “Evidence for truncated exponential probability distribution of earthquake slip”, *Bull. Seismol. Soc. Am.* 106(2016), 1802-1816.
- [12] MIYAKOSHI, K., et al., “Re-examination of scaling relationships of source parameters of the inland earthquakes in Japan based on the waveform inversion of strong motion data”, *Journal of Japan Association for Earthquake Engineering*, 15(2015), 141-156 (in Japanese).
- [13] INTERNATIONAL ATOMIC ENERGY AGENCY (IAEA), “Diffuse seismicity in seismic hazard assessment for site evaluation of nuclear installations”, *Safety Reports Series*, No.89(2016), <https://www-pub.iaea.org/MTCD/publications/PDF/Pub1727web-33787836.pdf>



Cadarache-Château, France, 14-16 May 2018

- 
- [14] MAI, P. M., and BEROZA, G. C., “Source scaling properties from finite-fault-rupture models”, *Bull. Seismol. Soc. Am.* 90(2000), 604-615.
  - [15] THINGBAIJAM, K. K. S., et al., “New empirical earthquake source-scaling laws”, *Bull. Seism. Soc. Am.* doi: 10.1785/0120170017 (2017).
  - [16] AKI, K., “Scaling law of seismic spectrum”, *J. Geophys. Res.* 72(1967), 1217-1231, doi:10.1029/JZ072i004p01217.
  - [17] BOUCHON, M., “The state of stress on some fault of the San Andreas system as inferred from near-field strong motion data”, *J. Geophys. Res.* 102(1997), 11731-11744.
  - [18] IDE, S., and TAKEO, M., “Determination of constitutive relations of fault slip based on seismic wave analysis”, *J. Geophys. Res.* 102(1997), 27379-27391.
  - [19] OKADA, Y., “Internal deformation due to shear and tensile faults in a half-space”, *Bull. Seismol. Soc. Am.* 82(1992), 1018-1040.
  - [20] IWATA, T., et al., “Dynamic source parameters for characterized source model for strong motion prediction”, *International Symposium on Earthquake Engineering Commemorating Tenth Anniversary of the 1995 Kobe Earthquake (ISEE Kobe 2005)*, Kobe and Awaji, A159-A164(2005).
  - [21] ASANO, K., and IWATA, T., “Characterization of stress drops on asperities estimated from the heterogeneous kinematic slip model for strong motion prediction for inland crustal earthquakes in Japan”, *Pure Appl. Geophys.* 168(2011), 105-116.
  - [22] FUJII, Y., and MATSU’URA, M., “Regional difference in scaling laws for large earthquakes and its tectonic implication”, *Pure Appl. Geophys.* 157(2000), 2283-2302.
  - [23] MAI, P. M., and THINGBAIJAM, K. K. S., “SRCMOD: An online database of finite-fault rupture models”, *Seism. Res. Lett.* 85(2014), 1348-1357.